Biogenic Synthesis of Silver Nanoparticles Mediated by the Consortium Comprising the Marine Fungal Filtrates of Penicillium Oxalicum and Fusarium Hainanense Along With Their Antimicrobial, Antioxidant and Larvicidal Potency

Rashmi Thakor
Hemchandracharya North Gujarat University
Harsh Mistry
Hemchandracharya North Gujarat University
Hitesh Patel
Hemchandracharya North Gujarat University
Himanshu S Bariya (hsbariya@ngu.ac.in)
Hemchandracharya North Gujarat University

Research Article

Keywords: Penicillium oxalicum, Fusarium hainanense, Consortium, Antioxidant activity, Antimicrobial activity, Larvicidal activity

Posted Date: December 3rd, 2021

DOI: https://doi.org/10.21203/rs.3.rs-1115139/v1

Abstract

The silver nanoparticles were biosynthesized using fungal isolates as well as their mixed cell free filtrate acting as a consortium namely, DS-2 (*Penicillium oxalicum*), DW-8 (*Fusarium hainanense*) and DSW-28, respectively. The UV-Visible spectra determined the surface plasmon resonance at 438, 441 and 437 nm for the silver nanoparticles synthesized by DS-2, DW-8 and DSW-28, respectively. The Tauc's plot analysis disclosed the band gap energy between 2.21 eV to 2.24 eV which depicted their ability to act as a semiconductor. The TEM imaging revealed the spherical shape along with the average particle size of DS-2 as 11.14 ± 2.39 nm and DW-8 as 7.59 ± 1.31 nm whereas that of DSW-28 as 5.73 ± 0.4 nm. Thus, the silver nanoparticles synthesized by DSW-28 were smaller in size than the individual isolates. The XRD pattern of the silver nanoparticles exhibited the crystalline structure corresponding to their peaks. The FTIR spectra indicates the presence of different functional groups on the surface of the synthesized silver nanoparticles. The broad-spectrum antimicrobial activity was exhibited by silver nanoparticles synthesized by DSW-28 against Gram positive, Gram negative bacteria and plant pathogen *Fusarium oxysporum* than the individual fungal isolates. The DSW-28 synthesized silver nanoparticles also acts as an effective antioxidant by depicting their radical scavenging activity against DPPH. Moreover, the silver nanoparticles synthesized by DSW-28 also inhibited the growth of 4^{th} instar larvae of *Aedes aegypti* and *Culex quinquefasciatus* more efficiently than DS-2 and DW-8 in a dose-dependent method. The impressive bioactivity of the silver nanoparticles synthesized by the mixture of cell free filtrate of various fungi acting as a consortium recommends their prospective use in agriculture as well as in biomedical as an antimicrobial, antioxidant and larvicidal agents in future.

Highlights

- First report on green synthesis of silver nanoparticles using consortium developed using two marine derived fungi *Penicillium oxalicum and Fusarium hainanense.*
- Biosynthesized silver nanoparticles were stable at room temperature for more than 6 months.
- Antibacterial effect of nanoparticles on three Gram-positive and two Gram-negative bacteria due to their synergistic effects.
- Antifungal effect of nanoparticles against plant pathogenic fungi *Fusarium oxysporum*
- Antioxidant activity of silver nanoparticles using DPPH.
- Larvicidal activity of silver nanoparticles against 4^{th} instar larvae of *Aedes aegypti* and *Culex quinquefasciatus*

Introduction

Nanoscience explicit a prospering field offering a better future which deals with the nano-sized material within the range of 1-100 nm with varied properties conceding them immense potentials that can be utilized in diverse applications like agriculture, pharmaceutical, healthcare and medicine [1]. Amidst all metallic nanoparticles, silver nanoparticles are significantly utilized for their broad-spectrum

antimicrobial, antioxidative, anticancer as well as larvicidal potentiality [2, 3, 4]. Synthesis of silver nanoparticles by chemical and physical techniques pose several drawbacks such as utilizing high raw materials, requiring high temperature and discharging toxic by-products which can be considered hazardous for both human health as well as agriculture [5, 6]. Moreover, the production of silver nanoparticles by biological method using natural sources such as plants, fungi, bacteria, algae, archaea etc. provides an easy, cost-effective and ecologically non-perilous alternative for their large-scale synthesis. This technique imparts stability and facilitates the fabrication of silver nanoparticles with desired size and morphology [4, 7].

Fungi tends to be more ideal for the biogenic synthesis of silver nanoparticles as they are easy to handle and harvest in bulk amount, possess high tolerance towards the metal, secrete higher amount of the unique extracellular proteins and other biomolecules which acts as a reducing as well as capping agents responsible for the stability nanoparticles [6, 8]. Besides this, the development of a consortium using cell free filtrate from different fungal strains provides a novel and unique approach for the biological synthesis of the silver nanoparticles. The utilization of mixed cell free filtrate from different fungi enhances the biofabrication of silver nanoparticles efficiently than the individual isolates with better stability, smaller particle size and higher bioactivity as they possess variety of biomolecules from different fungal sources [9, 10].

In the present study, the fungal isolates were screened out for the synthesis of silver nanoparticles. The cell free filtrate of two best screened out fungi namely DS-2 (*Penicillium oxalicum*) and DW-8 (*Fusarium hainanense*) were utilized in equal volumes as a consortium DSW-28 for the production of silver nanoparticles. The biosynthesized silver nanoparticles using both the individual fungal isolates (DS-2, DW-8) as well as mixed filtrate (DSW-28) were further characterized by UV-Visible and FTIR spectroscopic analysis, TEM imaging and XRD. The Antimicrobial activity of the synthesized silver nanoparticles was carried out against the three-Gram positive, the two-Gram negative bacteria as well as the plant pathogenic fungi namely *Fusarium oxysporum*. Furthermore, the antioxidant and the larvicidal activity of the synthesized silver nanoparticles were also carried out considering them as an effective antimicrobial as well as mosquitocidal agents in future.

Experimental

Biosynthesis of Nanoparticles

The fungal isolates *Penicillium oxalicum* (DS-2) and *Fusarium hainanense* (DW-8) (GenBank accession number: MT647130 and MT647137) were grown in potato dextrose broth in shaking condition (120 rpm) for 96 h at 28 ºC. Harvested Biomass (6 g) was filtered through Whatman® filter paper no. 42 followed by washing with Milli-Q water and resuspended in 100 mL of Milli-Q water for 24 h at 60 ºC. The biomass was again filtered using Whatman® filter paper no. 42. The acquired cell free filtrate (CFF) was further utilized for the biogenesis of silver nanoparticles (AgNPs). For the biosynthesis of silver nanoparticles (AgNPs), 10 mL of CFF from each fungal strain (DS-2 and DW-8) and their mixture (DSW-28) in ratio of

1:1 v/v; (pH-9.0) was reacted with 90 mL of 10 mM silver nitrate solution ($AgNO_3$, M.W. 169.87, HiMedia) at 60 ºC in the water bath. The experiment was carried out in dark condition to avoid any photochemical reactions.

Characterization of mycosynthesized silver nanoparticles

Characterization of synthesized nanoparticles from monocultures (DS-2 and DW-8) and their consortium (DSW-28) were carried out using UV-Visible, X-ray diffraction (XRD), Attenuated total reflectance-Fourier transform infrared spectroscopy (ATR-FTIR) and Transmission electron microscopy (TEM). Biosynthesis of silver nanoparticles was analyzed using UV–Vis spectrophotometer (Shimadzu, UV-1800 series) and absorption spectra were measured in the range of 300 nm to 700 nm. Morphological study (Shape and size) of the synthesized AgNPs were analyzed by TEM. The surface chemistry of the sample was studied using ATR-FTIR. Analysis of diffraction patterns were carried out using X-ray diffractometer. CuKα radiation with a wavelength of 1.5406 nm was recorded in the 2θ range from 0º to 90º and operated at 30 kV and 100 mA. Band gap energy (Eg) of nanoparticles was calculated by using Tauc's plot.

Antimicrobial activity of silver nanoparticles (AgNPs)

Antimicrobial activity of synthesized AgNPs was carried out against three Gram-positive (*B. subtilis, B. megaterium* and *S. aureus*), two Gram-negative bacteria (*P. aeruginosa* and *E. coli*) and the Plant pathogenic fungi *Fusarium oxysporum*. The antibacterial activity was carried out via a well diffusion method. Bacterial strains were grown in nutrient broth at 37 ºC for 24 h and were adjusted to 0.5 as per McFarland standards. 100 µL of bacterial suspension was spread on a nutrient agar plate using a glass spreader under sterile conditions. A 12 mm diameter well was punched on the nutrient agar plate using a cork borer and the synthesized AgNPs and $AgNO_3$ were inoculated in each well. Similarly, 100 µL of ampicillin (1 mg/mL) served as a positive control. All the plates were incubated at 37 °C for 24 h and the antibacterial activity was evaluated by measuring the diameter of the inhibition zone using zone scale (HiMedia). Antifungal activity of AgNPs was performed using plant pathogenic fungal strain *Fusarium oxysporum*. Fungal suspension (10^6 spores/mL) was spread on potato dextrose agar plate and a 12 mm diameter well was punched on the agar plate using a cork borer and the synthesized AgNPs and $AgNO_3$ were inoculated in each well. Similarly, 100 µL of fluconazole (1 mg/mL) served as a positive control. The plates were incubated at 28 °C for 72 h and the antifungal activity was evaluated by measuring the diameter of the inhibition zone using zone scale (HiMedia) [11].

Antioxidant activity by 2,2-diphenyl-1- picrylhydrazyl (DPPH) method

The antioxidant potency of synthesized AgNPs was tested using the method described by [12] with minor modifications. The DPPH test was used to assess the radical scavenging activity of AgNPs. Various concentrations (10, 20, 30, 40, 50, 75, and 100 µg/mL) of 1 mL AgNPs were vortexed with 1 mL of freshly prepared 1 mM DPPH solution. The solution was then maintained in the dark for 30 min at room temperature. At 517 nm, the absorbance was measured. As a control, DPPH with all reagents except the sample was utilized, and methanol was used as a blank.

Mosquito rearing and Larvicidal activity of AgNPs

Aedes aegypti and *Culex quinquefasciatus* were collected from ICMR- National Institute of Malaria Research, Nadiad, Gujarat, India in February - 2021 and have been maintained under aseptic and suitable environmental conditions (relative humidity: 80 ± 10%, temperature: 28 ± 1ºC, photoperiod: 16:8 h light/dark cycle) in insectarium. The larvae were hatched until reaching the 4^{th} instar and then were used for larvicidal activity. 25 4^{th} instar larvae were placed in 200 mL of the test solution with various concentrations of silver nanoparticles (10, 25, 50 and 100 ppm) under preceding conditions. During this time period, no food supplements were provided and mortality was determined 24 h after the initiation of each bioassay. Larvae were termed as dead when the larvae either did not move, showed slow movement or were unable to rise to the surface of medium.

Statistical analysis

Statistical analysis was accomplished using IBM SPSS Statistics 23. All the experimental values were expressed as a mean ± SE. Significance level also indicated after performing 1 way ANOVA analysis. All the graphical representations were prepared in Origin 2021 (9.8) and MedCalc (version 20.015) [4, 10].

Results And Discussion

Penicillium oxalicum (DS-2) and *Fusarium hainanense* (DW-8) were isolated from soil and water sample, respectively, collected from the sea coast of Diu, India (20°42'17.3" N 70°54'55.8" E), and were subjected to AgNPs biosynthesis (Fig. 1). The CFF of *Penicillium oxalicum* (DS-2), *Fusarium hainanense* (DW-8) and their consortium (DSW-28) was reacted with 10 mM $AgNO_3$ solution in a 9:1 (v/v) ratio. The addition of $AgNO_3$ to the CFF of *Penicillium oxalicum* (DS-2), *Fusarium hainanense* (DW-8) and their consortium (DSW-28) resulted in an immediate change in solution color from colorless to light yellow, followed by a change to light brown at 12 h and a dark brown solution at 36 h as the reaction progressed, as shown in Figure 2.

UV-Visible spectroscopic analysis

A UV–Visible spectrophotometer was used to monitor the continuous formation of AgNPs. The synthesized CFF reduced AgNPs that had shown a unique absorption peak attributing to their surface plasmon resonance [13]. The absorption peak for DS-2, DW-8, and DSW-28 in the UV–visible spectrum of an aqueous medium containing silver nanoparticles was with 438, 441, and 437 nm, respectively. With the increasing incubation time, the intensity of the absorption peaks was increased. Even after 72 hours of incubation, there has been no change in the location of the absorption peak (Table 1), indicating that the AgNPs have a uniform particle shape [14]. Furthermore, it is proven that the synthesis of highly dense nanoparticles is responsible for enhancing the intensity of absorption peaks [15]. The results have been found to be consistent with the findings of many other researchers around the world. Figure 3 indicates that the SPR of synthesized AgNPs has not shown any change after 6 months (stored at room temperature).

Band gap energy by Tauc's plot

A semiconductor's band gap energy describes the amount of energy required to excite an electron from the valence band to the conduction band. The Tauc's plot proposed using optical absorption spectra was to estimate the band gap energy of amorphous semiconductors in 1966 [16]. The band gap energy (Eg) of all the three synthesized AgNPs was then estimated by extrapolating linear section of the curve (UV-Visible spectra) from Tauc's plot. The AgNPs of DS-2, DW-8, and DSW-28 achieved band gap energies of 2.21, 2.24, and 2.21 eV, respectively, in Figure 4. As a semi-conductive material, these particles with enormous band gap energies can be employed in advanced optoelectronic devices, batteries, and sensors. The band gap value is quite comparable to what has previously been reported in the literature, and it is possible that this value is attributable to the quantum confinement effect [4, 17].

Fourier-transform infrared spectroscopic (FTIR) analysis

Figure 5 depicts the FTIR spectrum of synthesized AgNPs, which shows absorption peaks in the 4000 cm^{-1} to 500 cm^{-1} range. The absorption bands in the FTIR spectra of DS-2 were found to be 3265 cm^{-1}, 2127 cm^{-1}, 1661 cm^{-1}, and 760 cm^{-1}. Absorption bands observed for DW-8 were at 3298 cm^{-1}, 2135 cm^{-1}, 1662 cm^{-1}, and 745 cm^{-1}, whereas the absorption bands observed for their mixed CFF (DSW-28) were at 3266 cm^{-1}, 2093 cm^{-1}, 1660 cm^{-1}, and 744 cm^{-1}. The FTIR peaks at various location in the region of 4000 cm^{-1} to 500 cm^{-1} indicate the presence of capping and stabilizing biomolecules on the nanoparticles' surface. Dr. Friedrich Menges' software SpectraGryph (version 1.2) was used to analyze ATR-FTIR spectra. Table 2 shows the peaks and their corresponding functional groups, which concurred with the research results of several researchers throughout the world.

At optimum conditions, the incorporation of silver salt into CFF solution results in immediate binding of silver ions with the protein and other molecules present in CFF solution with functional groups such as –OH and C=C being captured, resulting in conformational changes in proteins that represent its hydrophobic residues to the aqueous phase, resulting in infiltration of reducing agents from CFF solution and thus providing capping to silver ions with the formation of stable nanoparticles [18, 19]. Assuming the CFF of the marine fungi *Penicillium oxalicum* and *Fusarium hainanense* used in this study, it is conceivable that alkyne, sulfurous and phenolic compounds, proteins, alcohol and other water-soluble biomolecules contributed as reducing and stabilizing agents to the silver nanoparticles [5, 20].

X-ray diffraction analysis

Figure 6 depicts the distinct XRD patterns of mycosynthesized AgNPs by DS-2, DW-8 and DSW-28. XRD pattern of DS-2 exhibited diffraction peaks corresponding to [111], [200], [220] and [311] appearing at 2θ representing the value of 37.89°, 44.19°,64.22° and 77.11°, respectively. XRD pattern of DW-8 exhibited diffraction peaks corresponding to [110], [111], [200] and [220] appearing at 2θ representing the value of 33.18°, 37.76°,46.74° and 66.12°, respectively. The XRD pattern of consortium DSW-28 exhibited diffraction peaks corresponding to [110], [111], [200]and [311] appearing at 2θ representing the value of

33.31°, 38.11°, 44.2° and77.6°, respectively. In accordance with COD ID no. 1100136, these peaks represent crystallographic planes of face-centered cubic (fcc) Ag. The Debye-Scherrer formula was used to calculate the mean particle size of AgNPs [21].

$$D = \frac{0.9\lambda}{\beta \cos \theta}$$

Where,

D represents the crystalline size (nm),

Λ indicates the wavelength of X-ray (0.1541 nm),

β specifies the angular line full width at half maximum (FWHM) of the peak (in radians) and

θ displays the Braggs angle (in radians)

As indicated in Table 3, the mean size of the silver nanoparticles was estimated to be from 14.19 ± 3.14 nm, 8.87 ± 2.31 nm, and 5.14 ± 0.99 nm for DS-2, DW-8, and DSW-28, respectively. The nanocrystalline nature of the mycosynthesized NPs is attested by the extensive pattern of the XRD diffraction peaks [7].

Transmission Electron Microscopic (TEM) analysis

As shown in Figure 7, TEM analysis demonstrated the synthesis of nanocrystalline silver particles. AgNPs with a spherical morphology and uniform size of 11.14 ± 2.39 nm, 7.59 ± 1.31 nm, and 5.73 ± 0.4 nm of DS-2, DW-8, and DSW-28, respectively, were observed. Particles of larger sizes were found in the sample in exceptional cases, although in small proportions. The presence of lattice fringes in the TEM images of synthesized AgNPs demonstrated their crystalline structure, with the 'd' spacing values correlating to the X - ray diffraction patterns. Furthermore, the selected area electron diffraction (SAED) pattern exhibited ring patterns with single spots in a ring (Fig. 7) that are consistent with the XRD patterns. Figure 8 shows the TEM-derived size distribution curve. The nanoparticles with the size range of 5.19 to 21.3 nm for DS-2, 3.04 to 13.5 nm for DW-8, and 1.5 to 17.3 nm for DSW-28 were obtained according to TEM analysis. Until now, a larger size range of AgNPs produced employing various fungus and plant extracts has also been described [13, 22, 23].

Antimicrobial activity of AgNPs

The antimicrobial potential of AgNPs was assessed by measuring the inhibition zone diameter and the observations are shown in Table 4 and Table 5. In this study, the highest zone of inhibition had been observed against Gram-positive bacteria compared to the Gram-negative bacteria. The prospect of employing these AgNPs as a broad-spectrum antimicrobial agent was clearly recognized by these results. This experiment is in correspondence with the view of Mistry et al. (2021) [4] that the probable antimicrobial potential of AgNPs is because of their higher surface-to-volume ratio and their crystalline structure [24]. The AgNPs have been found to rupture the cell membrane, resulting in the generation of

reactive oxygen species (ROS) that damage the DNA and proteins, followed by the microorganism's destruction [25]. Many previous studies have reported that AgNPs are more hazardous to the Gram-negative bacteria than Gram-positive bacteria since they have a thinner peptidoglycan layer through which AgNPs can infiltrate and disrupt their proteins and DNA, ultimately leading to microbial death. Conversely, higher amount of nanoparticles are required to show antibacterial potency against gram positive bacteria as they contain thicker peptidoglycan layer [26]. As a consequence, AgNPs aren't highly effective against Gram-positive microorganisms. However, AgNPs synthesized by DS-2, DW-8 and DSW-28 showed very effective results against Gram-positive bacteria (Table 4). *Fusarium oxysporum* is a plant pathogenic fungus known to cause wilt in many ecologically important plants like cumin, banana that leads to yield loss [27, 28]. To overcome this issue, *Fusarium oxysporum* was treated by AgNPs synthesized from DS-2, DW-8 and DSW-28. Results obtained after incubation period of 72 h has shown intensive antifungal potential of AgNPs. Zone of inhibition of mixed CFF DSW-28 was higher (19 ± 0.32 mm) in comparison of DS-2 (13 ± 0.33 mm), DW-8 (15 ± 0.31 mm), standard fluconazole (12 ± 0.17 mm) and 10 mM $AgNO_3$ solution (11 ± 0.35 mm) (Table 5). In this study interestingly, AgNPs derived from mixed CFF of marine fungi *Penicillium oxalicum* and *Fusarium hainanense* were found to be impressively effective against Gram-positive as well as Gram-negative bacteria and plant pathogenic fungal strain in compare of their individual CFF (DS-2 and DW-8). In mixed CFF, presence of various precious biometabolites from both the fungi could be responsible for higher bioactivity towards human as well as plant pathogens. This characteristic of mycosynthesized AgNPs will contribute in the advancement of broad-spectrum antimicrobial activity [5].

Antioxidant capacity of CFF derived AgNPs

DPPH is a stable molecule that can be reduced by admitting hydrogen or electrons, and it has been extensively utilized to assess antioxidant properties of the silver nanoparticles. In this experiment, various concentrations of biosynthesized AgNPs were reacted with DPPH reagent to assess their antioxidative potency. As a result, AgNPs synthesized by marine fungal cell free filtrate DS-2 and DW-8 and their consortium DSW-28 have shown effective antioxidant potential as their radical scavenging ability was increasing with the increment in their concentration. Figure 9 shows the antioxidant activity of the AgNPs. Their IC_{50} value was calculated in Microsoft excel-2019 which was about 71.33 (µg/mL) for DS-2, 61.30 (µg/mL) for DW-8 and DSW-28 was about 42.56 (µg/mL). Above mentioned results confirmed that the AgNPs synthesized by mixing their CFF have more antioxidative properties than AgNPs synthesized using their individual CFF which were DS-2 and DW-8 as they possess lower IC_{50}.Antioxidative potential of the silver nanoparticles is due to the adsorption of fungal constituents from CFF on the silver nanoparticle [12]. Metal nanoparticles produced by marine fungi exhibit a wide range of biological activities, including antioxidant, antibacterial, and antimalarial properties. Marine fungus like *Aspergillus brunneoviolaceus* and *Cladosporium cladosporioides* have recently been found to produce AgNPs with excellent antioxidant activity. The findings significantly support the use of AgNPs as natural antioxidants for health protection against a wide range of oxidative stressors associated with degenerative diseases. This antioxidant

validation is essential for synthesized AgNPs before their utilization against experimental models such as mice or against humans [4, 24, 29, 30].

Larvicidal activity of silver nanoparticles

The synthesized AgNPs from DS-2, DW-8 and DSW-28 were exposed against 4th instars larvae of *Aedes aegypti* and *Culex quinquefasciatus* at various concentrations (10–100 µg/mL) for 24 h. Amongst all, the AgNPs synthesized from mixed CFF of DS-2 and DW-8 which is DSW-28 had exhibited potent larvicidal activity. Figure 10 depicts the dose response plot of AgNPs against larvae of *Aedes aegypti* and *Culex quinquefasciatus.* The maximum mortality rate observed for DSW-28 was 88% and 92% with LC_{50} values of 35.37 and 13.35 µg/mL against *Aedes aegypti* and *Culex quinquefasciatus*, respectively (Fig-10). Distilled water was taken as a control. No mortality of any larvae was observed in control groups. The mortality rate was significantly augmented with an increasing dose-dependent manner where the highest mortality rate was observed with the increasing concentrations of synthesized AgNPs. This difference in lethal concentrations might be due to differences in secondary metabolites present in the fungi. It has been reported that AgNPs are responsible for impeding the process of food consumption development in mosquito young instar resulting in their death. Furthermore, AgNPs can easily penetrate into the exoskeleton of larvae and attach to the sulfur or phosphorus containing biomolecules like proteins, DNA and RNA which leads to the quick denaturation of organelles and enzymes which could be the possible reason for the death of mosquito larvae. Due to the disturbance in proton motive force important for ATP construction and decreased permeability of membrane by AgNPs, cellular functions may not work properly and cell will die [31, 32, 33]. AgNPs synthesized from DSW-28 had shown highest rate of mortality against both the larvae. Reason behind that characteristic of DSW-28 could be synergistic effect of both the fungal metabolites present and attached on the surface of nanoparticles [10].

Conclusion

A novel approach of synthesizing silver nanoparticles using the mixture of cell free filtrate of different fungi has been demonstrated in this study. The biogenic silver nanoparticles were spherical in shape with the average particle size of 5.73 ± 0.4 nm displaying maximum surface by volume ratio exhibiting better biopotentials compared to the silver nanoparticles synthesized by individual isolates. The broad-spectrum antimicrobial activity of the synthesized nanoparticles against bacteria as well as plant pathogenic fungi revealed their potentiality in both medicine as well as agriculture. The synthesized silver nanoparticles displayed their efficient antioxidative potentiality against DPPH and also larvicidal activity by ceasing the growth of 4th instar larvae of *Aedes aegypti* and *Culex quinquefasciatus*. Thus, the study unfolds the unique perspective of using the mixture of cell free filtrate of different fungi for the effective synthesis of silver nanoparticles with desired size and bio-potentialities in diverse fields.

Declarations

Acknowledgements

The Authors highly acknowledge the Department of Biotechnology and Department of Life Sciences for providing the research facilities.

Funding

This research did not receive any specific grant from funding agencies in the public, commercial, or not-for-profit sectors.

Contribution

Rashmi Thakor: Conceptualization, Validation, Writing-review and editing, Writing-original draft

Harsh Mistry: Writing-review and editing, Writing-original draft, Data curation, Formal analysis

Hitesh Patel: Methodology, Resources

Himanshu Bariya: Methodology, Writing-original draft**,** Project administration, Investigation

Corresponding author

Correspondence to Himanshu Bariya

Ethics declarations

Conflict of interest

The authors confirm that the content of this manuscript has no conflict of interest.

Ethical Approval

Not applicable

Consent to Participate

Not applicable

Consent to Publish

All authors have read and approved the final drafted manuscript.

References

1. M.A. Yassin, A.M. Elgorban, A.E.-R. El-Samawaty, B.M.A. Almunqedhi, Biosynthesis of silver nanoparticles using *Penicillium verrucosum* and analysis of their antifungal activity. Saudi. J. Biol. Sci. **28**, 2123 (2021). doi:10.1016/j.sjbs.2021.01.063

2. Y.Y. Loo, Y. Rukayadi, M.-A.-R. Nor-Khaizura, C.H. Kuan, B.W. Chieng, M. Nishibuchi, S. Radu, In vitro antimicrobial activity of green synthesized silver nanoparticles against selected gram-negative foodborne pathogens. Front. Microbiol. 9, (2018). doi:10.3389/fmicb.2018.01555
3. P.K. Seetharaman, R. Chandrasekaran, S. Gnanasekar, G. Chandrakasan, M. Gupta, D.B. Manikandan, S. Sivaperumal, Antimicrobial and larvicidal activity of eco-friendly silver nanoparticles synthesized from endophytic fungi *Phomopsis liquidambaris*. Biocatal. Agric. Biotechnol. **16**, 22 (2018). doi:10.1016/j.bcab.2018.07.006
4. H. Mistry, R. Thakor, C. Patil, J. Trivedi, H. Bariya, Biogenically proficient synthesis and characterization of silver nanoparticles employing marine procured fungi *Aspergillus brunneoviolaceus* along with their antibacterial and antioxidative potency. Biotechnol. Lett. **43**, 307 (2021). doi:10.1007/s10529-020-03008-7
5. M. Guilger-Casagrande, R. de Lima, Synthesis of silver nanoparticles mediated by fungi: A Review. Front. Bioeng. Biotechnol. 7, (2019). doi:10.3389/fbioe.2019.00287
6. F. Ameen, A.A. Al-Homaidan, A. Al-Sabri, A. Almansob, S. AlNAdhari, Anti-oxidant, anti-fungal and cytotoxic effects of silver nanoparticles synthesized using marine fungus *Cladosporium halotolerans*. Appl. Nanosci. (2021). doi:10.1007/s13204-021-01874-9
7. X.-F. Zhang, Z.-G. Liu, W. Shen, S. Gurunathan, Silver nanoparticles: Synthesis, characterization, properties, applications, and therapeutic approaches. Int. J. Mol. Sci. **17**, 1534 (2016). doi:10.3390/ijms17091534
8. V. Netala, M. Bethu, B. Pushpalatha, V. Baki, S. Aishwarya, J. Rao, V. Tartte, Biogenesis of silver nanoparticles using endophytic fungus *Pestalotiopsis microspora* and evaluation of their antioxidant and anticancer activities. Int. J. Nanomedicine **11**, 5683 (2016). doi:10.2147/ijn.s112857
9. R. P., S. P., V. J., S. T., S. D.N.P., A. K., and D. R., Green synthesis of silver nanoparticles by *Aspergillus* consortium and evaluating its anticancer activity against human breast adenocarcinoma cell line (MCF7). Pharm. Biol. Eval. 4, 28 (2017). doi: 10.26510/2394-0859.pbe.2017.05
10. R. Thakor, H. Mistry, K. Tapodhan, H. Bariya, Efficient biodegradation of Congo red dye using fungal consortium incorporated with *Penicillium oxalicum* and *Aspergillus tubingensis*. Folia Microbiol. (Praha) (2021). doi:10.1007/s12223-021-00915-8
11. J.S. Pawar, R.H. Patil, Green synthesis of silver nanoparticles using *Eulophia Herbacea* (lindl.) tuber extract and evaluation of its biological and catalytic activity.SN Appl. Sci. 2, (2019). doi:10.1007/s42452-019-1846-9
12. A.K. Keshari, R. Srivastava, P. Singh, V.B. Yadav, G. Nath, Antioxidant and antibacterial activity of silver nanoparticles synthesized by *Cestrum nocturnum*. J. Ayurveda Integr. Med. **11**, 37 (2020). doi:10.1016/j.jaim.2017.11.003
13. R.M. Elamawi, R.E. Al-Harbi, A.A. Hendi, Biosynthesis and characterization of silver nanoparticles using *Trichoderma longibrachiatum* and their effect on phytopathogenic fungi. Egypt. J. Biol. Pest Control. 28, (2018). doi:10.1186/s41938-018-0028-1

14. T. Wu, F. Lu, Q. Wen, K. Yu, B. Lu, B. Rong, F. Dai, G. Lan, Novel strategy for obtaining uniformly dispersed silver nanoparticles on soluble cotton wound dressing through carboxymethylation and in-situ reduction: Antimicrobial activity and histological assessment in animal model. Cellulose <background-color:#FFCC66;bvertical-align:super;>25</background-color:#FFCC66;bvertical-align:super;>, 5361 (2018). doi:10.1007/s10570-018-1907-z
15. M.Z. Khan, F.K. Tarek, M. Nuzat, M.A. Momin, M.R. Hasan, Rapid biological synthesis of silver nanoparticles from *Ocimum sanctum* and their characterization. J. Nanosci. Nanotechnol. **2017**, 1 (2017). doi:10.1155/2017/1693416
16. J. Tauc, R. Grigorovici, A. Vancu, Optical properties and electronic structure of amorphous germanium. Physica Status Solidi (b) <background-color:#FFCC66;bvertical-align:super;>15</background-color:#FFCC66;bvertical-align:super;>, 627 (1966). doi:10.1002/pssb.19660150224
17. A.J. Das, R. Kumar, S.P. Goutam, Sunlight irradiation induced synthesis of silver nanoparticles using glycolipid bio-surfactant and exploring the antibacterial activity. J. Biomed. Eng. 06, (2016). doi:10.4172/2155-9538.1000208
18. A. Danagoudar, G.K. Pratap, M. Shantaram, K. Ghosh, S.R. Kanade, and C. G. Joshi, Characterization, cytotoxic and antioxidant potential of silver nanoparticles biosynthesised using endophytic fungus *(Penicillium citrinum* CGJ-C1). Mater. Today Commun. **25**, 101385 (2020). doi:10.1016/j.mtcomm.2020.101385
19. J. Osorio-Echavarría, J. Osorio-Echavarría, C.P. Ossa-Orozco, N.A. Gómez-Vanegas, Synthesis of silver nanoparticles using white-rot fungus anamorphous *Bjerkandera* sp. R1: Influence of silver nitrate concentration and fungus growth time. Sci. Rep. <background-color:#FFCC66;bvertical-align:super;>11</background-color:#FFCC66;bvertical-align:super;> (2021). doi:10.1038/s41598-021-82514-8
20. A.M. Othman, M.A. Elsayed, N.G. Al-Balakocy, M.M. Hassan, A.M. Elshafei, Biosynthesis and characterization of silver nanoparticles induced by fungal proteins and its application in different biological activities. J. Genet. Eng. Biotechnol. <background-color:#FFCC66;bvertical-align:super;>17</background-color:#FFCC66;bvertical-align:super;> (2019). doi:10.1186/s43141-019-0008-1
21. H. Bagur, R.S. Medidi, P. Somu, P.W. Choudhury, C.S. karua, P.K. Guttula, G. Melappa, C.C. Poojari, Endophyte fungal isolate mediated biogenic synthesis and evaluation of biomedical applications of silver nanoparticles. Mater. Technol. <background-color:#FFCC66;bvertical-align:super;>1</background-color:#FFCC66;bvertical-align:super;> (2020). doi:10.1080/10667857.2020.1819089
22. P.K. Kaman, P. Dutta, Synthesis, characterization and antifungal activity of biosynthesized silver nanoparticle. Indian Phytopathol. **72**, 79 (2018). doi:10.1007/s42360-018-0081-4
23. A. Ashraf, S. Zafar, K. Zahid, M. Salahuddin Shah, K.A. Al-Ghanim, F. Al-Misned, S. Mahboob, Synthesis, characterization, and antibacterial potential of silver nanoparticles synthesized from

Coriandrum sativum L. J. Infect. Public Health **12**, 275 (2019). doi:10.1016/j.jiph.2018.11.002

24. M. Manjunath Hulikere, C.G. Joshi, Characterization, antioxidant and antimicrobial activity of silver nanoparticles synthesized using marine endophytic fungus- *Cladosporium cladosporioides*. Process Biochem. **82**, 199 (2019). doi:10.1016/j.procbio.2019.04.011
25. L. Xu, Y.-Y. Wang, J. Huang, C.-Y. Chen, Z.-X. Wang, H. Xie, Silver nanoparticles: Synthesis, medical applications and Biosafety. Theranostics <background-color:#FFCC66;bvertical-align:super;>10</background-color:#FFCC66;bvertical-align:super;>, 8996 (2020). doi:10.7150/thno.45413
26. C. Liao, Y. Li, S. Tjong, Bactericidal and cytotoxic properties of silver nanoparticles. Int. J. Mol. Sci. <background-color:#FFCC66;bvertical-align:super;>20</background-color:#FFCC66;bvertical-align:super;>, 449 (2019). doi:10.3390/ijms20020449
27. T. Damodaran, S. Rajan, M. Muthukumar, R. Gopal, K. Yadav, S. Kumar, I. Ahmad, N. Kumari, V.K. Mishra, S.K. Jha, Biological Management of banana *Fusarium* wilt caused by *Fusarium oxysporum* f. sp. *cubense* tropical race 4 using antagonistic fungal isolate CSR-T-3 (*Trichoderma reesei*). Front. Microbiol. <bvertical-align:super;>11</bvertical-align:super;>, (2020). doi: 10.3389/fmicb.2020.595845
28. K. Yadav, T. Damodaran, N. Kumari, K. Dutt, R. Gopal, M. Muthukumar, Characterization of *Trichoderma* isolates and assessment of antagonistic potential against *Fusarium oxysporum* f. sp. cumini. J. Appl. Hortic. **22**, 38 (2020). doi:10.37855/jah.2020.v22i01.08
29. G.H.A.S.S.A.N.M. SULAIMAN, A.T. H. I. B., HUSSIEN, and M. A. Y. S. O. O. N. M. SALEEM, Biosynthesis of silver nanoparticles synthesized by *Aspergillus flavus* and their antioxidant, antimicrobial and Cytotoxicity properties. Bull. Mater. Sci. **38**, 639 (2015). doi:10.1007/s12034-015-0905-0
30. M. Govindappa, M. Lavanya, P. Aishwarya, K. Pai, P. Lunked, B. Hemashekhar, B.M. Arpitha, Y.L. Ramachandra, V.B. Raghavendra, Synthesis and characterization of endophytic fungi, *Cladosporium perangustum* mediated silver nanoparticles and their antioxidant, anticancer and nano-toxicological study. BioNanoScience **10**, 928 (2020). doi:10.1007/s12668-020-00719-z
31. R.B. Salunkhe, S.V. Patil, C.D. Patil, B.K. Salunke, Larvicidal potential of silver nanoparticles synthesized using fungus *Cochliobolus lunatus* against *Aedes aegypti* (Linnaeus, 1762) and *Anopheles stephensi* Liston (Diptera; Culicidae). Parasitol. Res. **109**, 823 (2011). doi: 10.1007/s00436-011-2328-1
32. G. Benelli, Plant-mediated biosynthesis of nanoparticles as an emerging tool against mosquitoes of medical and veterinary importance: A Review. Parasitol. Res. <background-color:#FFCC66;bvertical-align:super;>115</background-color:#FFCC66;bvertical-align:super;>, 23 (2015). doi:10.1007/s00436-015-4800-9
33. L.D. Amarasinghe, P.A.S.R. Wickramarachchi, A.A.A.U. Aberathna, W.S. Sithara, C.R. De Silva, Comparative study on larvicidal activity of green synthesized silver nanoparticles and *Annonaglabra* (Annonaceae) aqueous extract to control *Aedes aegypti* and *Aedes albopictus* (Diptera: Culicidae). Heliyon <bvertical-align:super;>6</bvertical-align:super;>, (2020)

Tables

Table 1 UV–visible spectroscopy data

s/n	Time of incubation	DS-2		DW-8		DSW-28		Color change
		Peak intensity (Abs.)	λ max (nm)	Peak intensity (Abs.)	λ max (nm)	Peak intensity (Abs.)	λ max (nm)	
1	24 h	0.975	437	1.179	441	1.529	438	Light yellow to light brown
2	48 h	1.102	438	1.323	441	1.640	436	Light brown to dark brown
3	72 h	1.131	437	1.476	440	1.754	439	Dark brown
4	96 h	1.191	439	1.567	441	1.868	437	Dark brown
5	185 days	1.224	438	1.602	441	1.902	437	Dark brown

Table 2 Fourier-transform infrared spectroscopy (FTIR) interpretation

s/n	DS-2	DW-8	DSW-28	Stretching/Bond	Functional group	Reference
	Wave number (cm^{-1})	Wave number (cm^{-1})	Wave number (cm^{-1})			
1	3265	3298	3266	O-H stretching	Alcohol/Phenol	Thirunavoukkarsu et al. 2013
2	2127	2135	-	C≡C stretching	Alkyne	Saravanan et al. 2018
3	-	-	2093	C=S stretching	Sulfur compound	Kumar et al. 2014
4	1661	1662	1660	C-C/ C-N stretching	Alkene or amines	Koyyati et al. 2014
5	760	745	744	C-H bending	alkane	Jyoti et al. 2016

Table:3 X-ray diffraction interpretation

AgNPs	s/n	2θ	θ	FWHM	Crystallite Size D(nm)	D nm (Average)	(hkl)
DS-2	1	37.89	18.945	0.73	11.50	14.19 ± 3.14	111
	2	44.19	22.095	1.1	7.79		200
	3	64.22	32.11	0.63	14.88		220
	4	77.11	38.555	0.45	22.57		311
DW-8	1	33.18	16.59	1.41	5.85	8.87 ± 2.31	110
	2	37.76	18.88	0.72	11.61		111
	3	46.74	23.37	0.62	13.88		200
	4	66.12	33.06	2.28	4.15		220
DSW-28	1	33.31	16.655	1.76	4.71	5.14 ± 0.99	110
	2	38.11	19.055	1.28	6.56		111
	3	44.2	22.1	3.4	2.52		200
	4	77.6	38.8	1.5	6.79		311

Table: 4 Antibacterial activity of AgNPs against Gram-positive and Gram-negative bacteria

S/n	Microorganisms	DS-2 (100 µL)	DW-8 (100 µL)	DSW-28 (100 µL)	Ampicillin (1 mg/mL)	$AgNO_3$ (10 mM, 100 µL)
		ZOI* (mm)	ZOI* (mm)	ZOI** (mm)	ZOI* (mm)	ZOI** (mm)
1	*B. subtilis*	13 ± 0.30	14 ± 0.31	16 ± 0.21	10 ± 0.30	9 ± 0.29
2	*S. aureus*	12 ± 0.32	13 ± 0.30	15 ± 0.20	12 ± 0.33	11 ± 0.24
3	*P. aeruginosa*	14 ± 0.31	14 ± 0.28	16 ± 0.24	13 ± 0.32	9 ± 0.30
4	*E. coli*	14 ± 0.28	15 ± 0.29	17 ± 0.20	10 ± 0.30	8 ± 0.32
5	*B. megaterium*	12 ± 0.25	12 ± 0.26	19 ± 0.22	14 ± 0.31	8 ± 0.25

Average value with standard error ($p < 0.05$) of three set of experiments. Experiment performed in triplicate. ** indicate highly significance at $p<0.05$ and * indicate significant at $p<0.05$.

Table 5 Antifungal activity of AgNPs against plant pathogenic fungi *Fusarium oxysporum*

S/n	Microorganisms	DS-2 (100 µL)	DW-8 (100 µL)	DSW-28 (100 µL)	Fluconazole (1 mg/mL)	$AgNO_3$ (10 mM, 100 µL)
		ZOI* (mm)	ZOI* (mm)	ZOI** (mm)	ZOI* (mm)	ZOI** (mm)
1	*Fusarium oxysporum*	13 ± 0.33	15 ± 0.31	19 ± 0.32	12 ± 0.17	11 ± 0.35

Average value with standard error ($p < 0.05$) of three set of experiments. Experiment performed in triplicate. ** indicate highly significance at $p<0.05$ and * indicate significant at $p<0.05$.

Figures

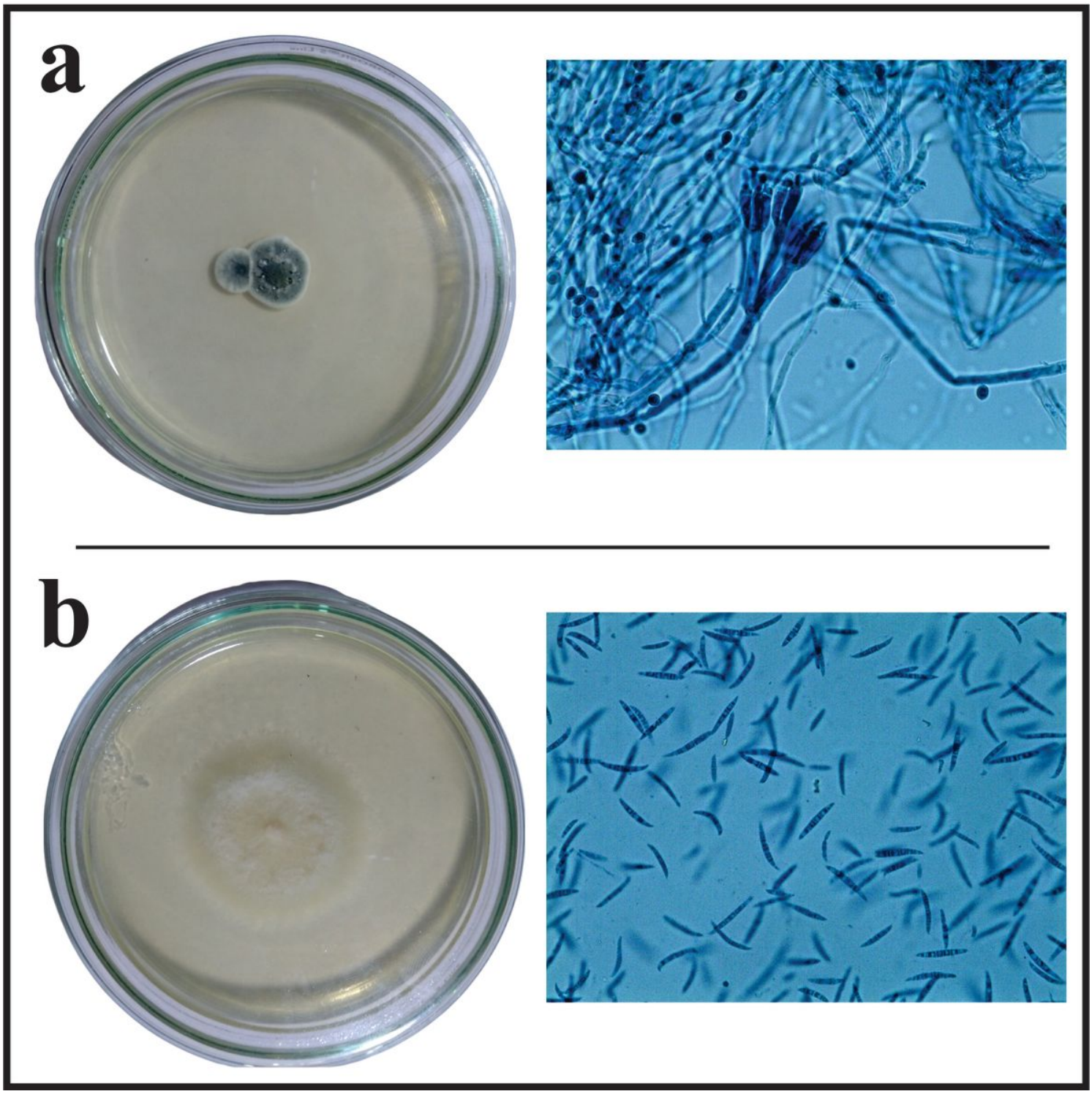

Figure 1

Penicillium oxalicum (a) and Fusarium hainanense (b) grown in Petri plate with growth medium along with its specific spore structure observed under microscope

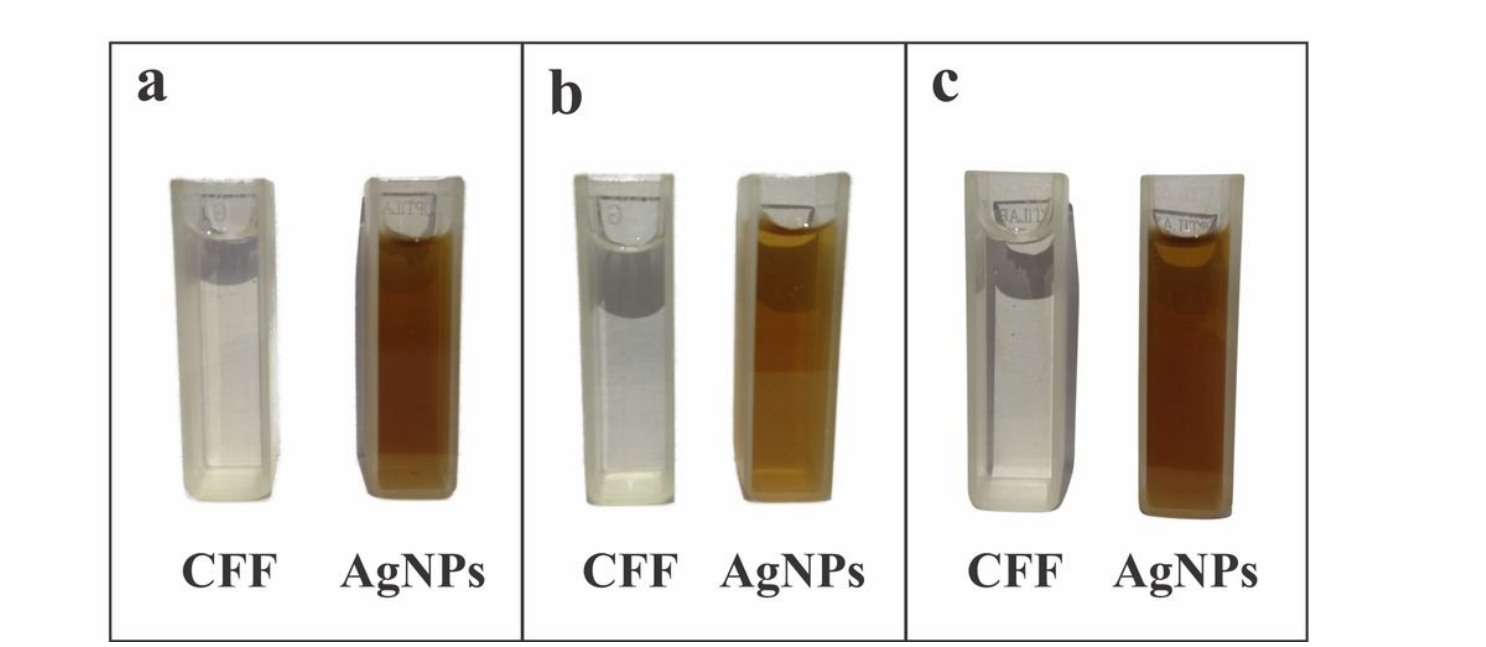

Figure 2

Primary visual identification of CFF and silver nanoparticles synthesized from DS-2 (a), DW-8 (b) and DSW-28 (c)

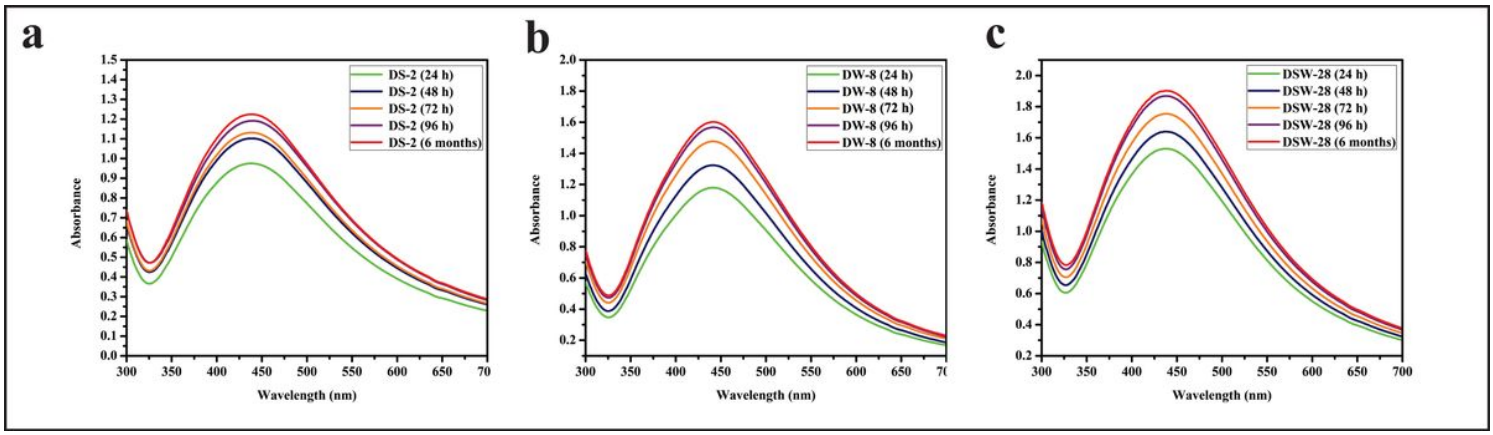

Figure 3

Absorbance maxima of silver nanoparticle synthesized from DS-2 (a), DW-8 (b) and DSW-28 (c) during different time intervals (24h, 48 h, 72 h, 96 h and 6 months).

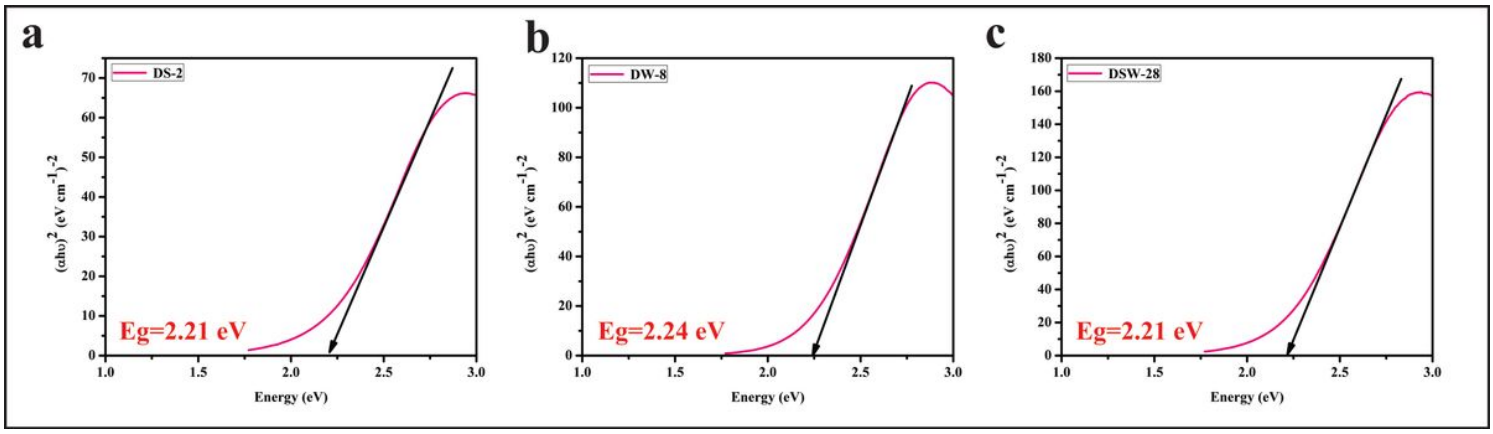

Figure 4

Band gap energy graph (Tauc's plot) of synthesized silver nanoparticle from DS-2 (a), DW-8 (b) and DSW-28 (c)

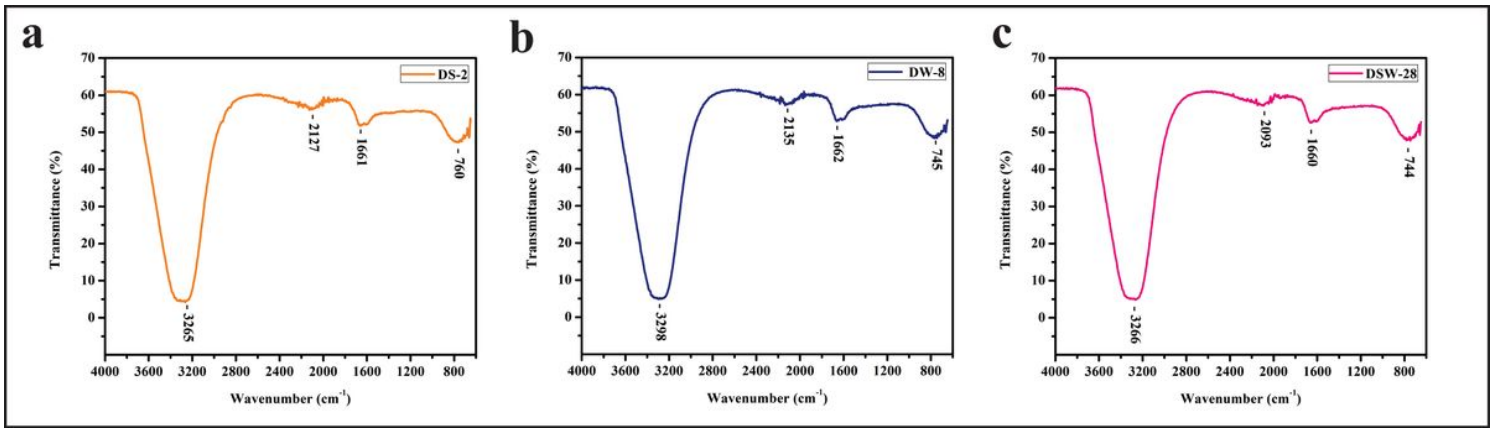

Figure 5

FTIR images of AgNPs synthesized from cell free filtrate of DS-2 (a), DW-8 (b) and DSW-28 (c). Different peaks in graph indicating presence of respective functional groups

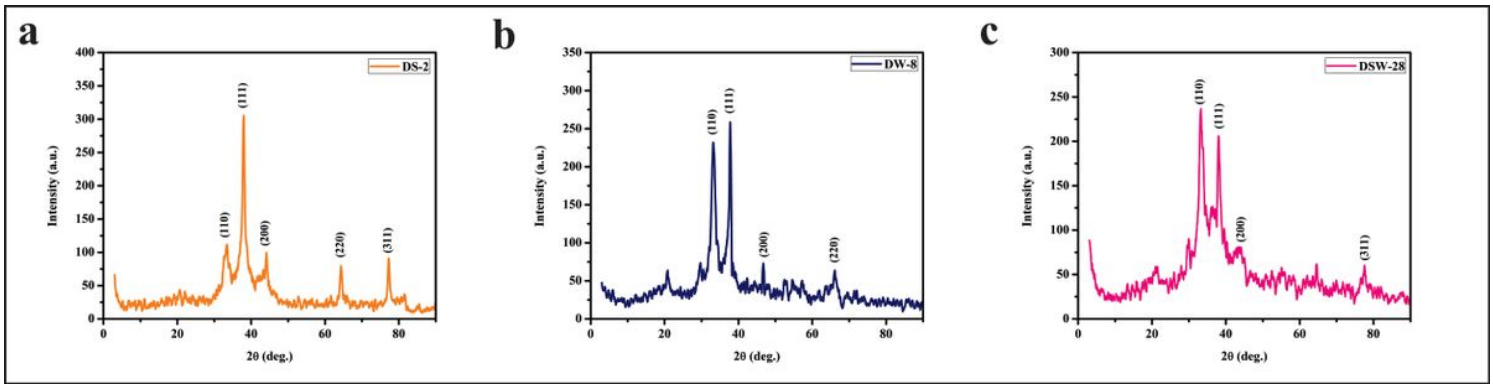

Figure 6

XRD pattern of AgNPs synthesized from cell free filtrate of DS-2 (a), DW-8 (b) and DSW-28 (c)

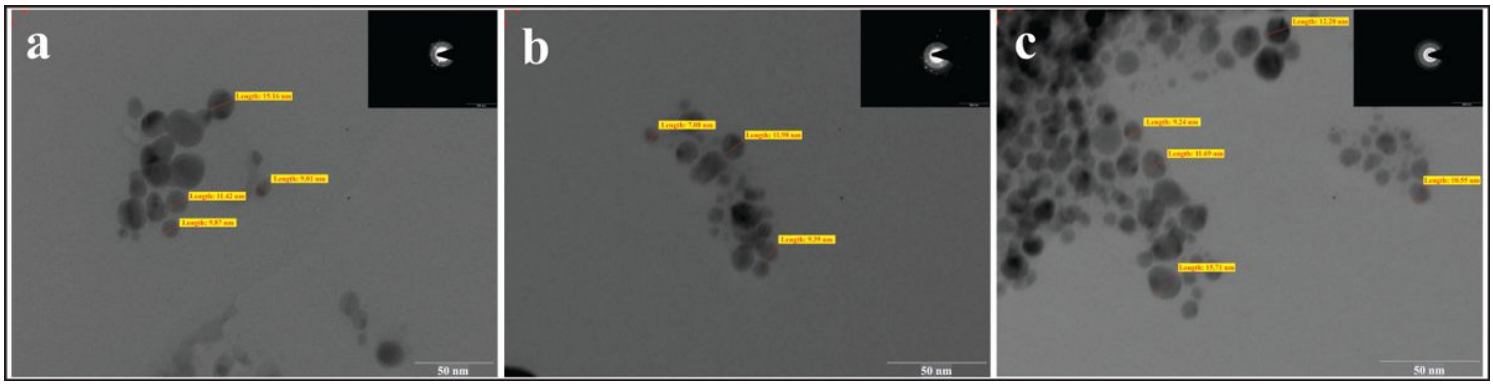

Figure 7

Synthesized silver nanoparticles from DS-2 (a), DW-8 (b) and DSW-28 (c) under Transmission electron microscope (TEM) and Selected area diffraction (SAED) pattern of AgNPs. Scale bar is 50 nm

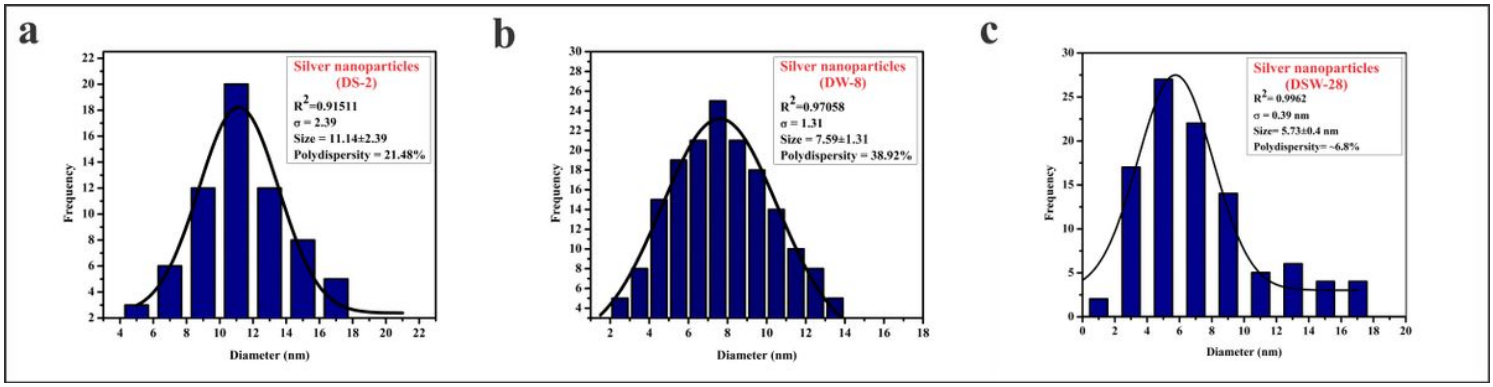

Figure 8

The size distribution curve from the TEM analysis and SAED pattern of synthesized silver nanoparticles from DS-2 (a), DW-8 (b) and DSW-28 (c)

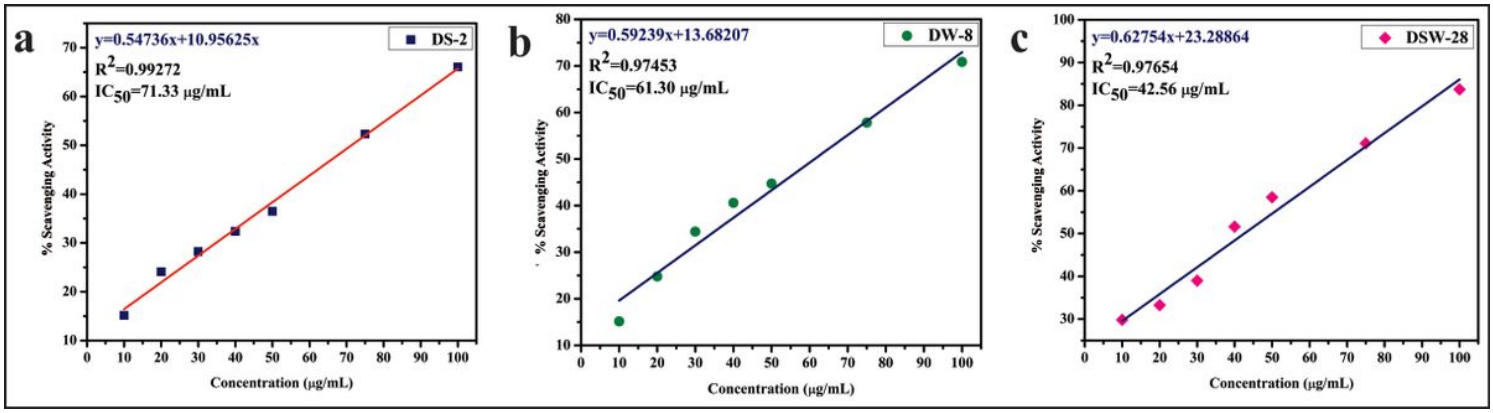

Figure 9

Antioxidant activity (%) of synthesized silver nanoparticle from DS-2 (a), DW-8 (b) and DSW-28 (c)

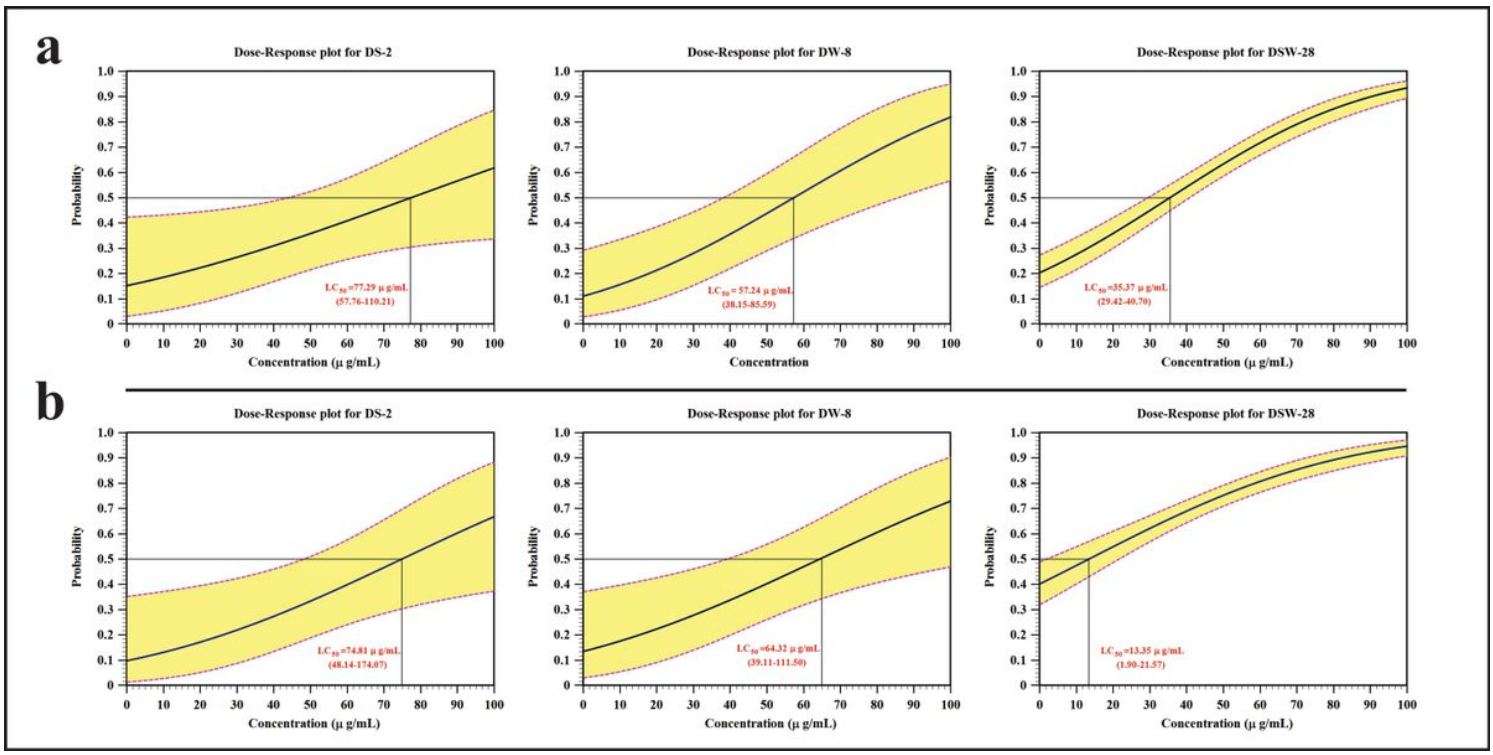

Figure 10

Dose-Response plot for DS-2, DW-8 and DSW-28 against Aedes aegypti (a) and Culex quinquefasciatus (b)

Supplementary Files

This is a list of supplementary files associated with this preprint. Click to download.

- GraphicalAbstract.jpg